

# The main-sequence rotation–colour relation in the Coma Berenices open cluster

A. Collier Cameron,<sup>1\*</sup> V. A. Davidson,<sup>1</sup> L. Hebb,<sup>1</sup> G. Skinner,<sup>1</sup> D. R. Anderson,<sup>2</sup> D. J. Christian,<sup>3</sup> W. I. Clarkson,<sup>4</sup> B. Enoch,<sup>1</sup> J. Irwin,<sup>5</sup> Y. Joshi,<sup>3</sup> C. A. Haswell,<sup>6</sup> C. Hellier,<sup>2</sup> K. D. Horne,<sup>1</sup> S. R. Kane,<sup>7</sup> T. A. Lister,<sup>8</sup> P. F. L. Maxted,<sup>2</sup> A. J. Norton,<sup>6</sup> N. Parley,<sup>6</sup> D. Pollacco,<sup>3</sup> R. Ryans,<sup>3</sup> A. Scholz,<sup>1</sup> I. Skillen,<sup>9</sup> B. Smalley,<sup>2</sup> R. A. Street,<sup>8</sup> R. G. West,<sup>10</sup> D. M. Wilson<sup>2</sup> and P. J. Wheatley<sup>11</sup>

<sup>1</sup>*SUPA, School of Physics and Astronomy, University of St Andrews, North Haugh, St Andrews, Fife KY16 9SS*

<sup>2</sup>*Astrophysics Group, School of Chemistry and Physics, Keele University, Staffordshire, ST5 5BG*

<sup>3</sup>*Astrophysics Research Centre, School of Mathematics and Physics, Queen's University, University Road, Belfast BT7 1NN*

<sup>4</sup>*STScI, 3700 San Martin Drive, Baltimore, MD 21218, USA*

<sup>5</sup>*Harvard-Smithsonian Center for Astrophysics, 60 Garden St, Cambridge, MA 02138, USA*

<sup>6</sup>*Department of Physics and Astronomy, The Open University, Milton Keynes MK7 6AA*

<sup>7</sup>*Michelson Science Center, Caltech, MS 100-22, 770 South Wilson Avenue, Pasadena, CA 91125, USA*

<sup>8</sup>*Las Cumbres Observatory, 6740 Cortona Dr. Suite 102, Santa Barbara, CA 93117, USA*

<sup>9</sup>*Isaac Newton Group of Telescopes, Apartado de Correos 321, E-38700 Santa Cruz de la Palma, Tenerife, Spain*

<sup>10</sup>*Department of Physics and Astronomy, University of Leicester, Leicester, LE1 7RH*

<sup>11</sup>*Department of Physics, University of Warwick, Coventry CV4 7AL*

Accepted 2009 July 30. Received 2009 July 30; in original form 2009 June 3

## ABSTRACT

We present the results of a photometric survey of rotation rates in the Coma Berenices (Melotte 111) open cluster, using data obtained as part of the SuperWASP exoplanetary transit-search programme. The goal of the Coma survey was to measure precise rotation periods for main-sequence F, G and K dwarfs in this intermediate-age ( $\sim 600$  Myr) cluster, and to determine the extent to which magnetic braking has caused the stellar spin periods to converge. We find a tight, almost linear relationship between rotation period and  $J - K$  colour with an rms scatter of only 2 per cent. The relation is similar to that seen among F, G and K stars in the Hyades. Such strong convergence can only be explained if angular momentum is not at present being transferred from a reservoir in the deep stellar interiors to the surface layers. We conclude that the coupling time-scale for angular momentum transport from a rapidly spinning radiative core to the outer convective zone must be substantially shorter than the cluster age, and that from the age of Coma onwards stars rotate effectively as solid bodies. The existence of a tight relationship between stellar mass and rotation period at a given age supports the use of stellar rotation period as an age indicator in F, G and K stars of Hyades age and older. We demonstrate that individual stellar ages can be determined within the Coma population with an internal precision of the order of 9 per cent (rms), using a standard magnetic braking law in which rotation period increases with the square root of stellar age. We find that a slight modification to the magnetic-braking power law,  $P \propto t^{0.56}$ , yields rotational and asteroseismological ages in good agreement for the Sun and other stars of solar age for which  $p$ -mode studies and photometric rotation periods have been published.

**Key words:** methods: data analysis – techniques: photometric – stars: activity – stars: rotation – open clusters and associations: individual: Melotte 111.

## 1 INTRODUCTION

In their pioneering study of stellar rotation among main-sequence stars in the Hyades open cluster, Radick et al. (1987) found a

\*E-mail: acc4@st-and.ac.uk

surprisingly narrow correlation between the  $B - V$  colours and the rotation periods of F, G and K stars. This discovery has several far-reaching implications. First, it confirms the theoretical prediction that the spin rates of an ensemble of stars of the same age and mass, but different initial rotation periods rates, should converge. This comes about because the rate at which angular momentum is lost through magnetic braking via a thermally driven, magnetically channelled wind, increases strongly as a function of stellar rotation rate (e.g. Mestel & Spruit 1987). Radick et al. showed that this convergence is essentially complete at the  $\sim 600$  Myr age of the Hyades. Secondly, for convergence to occur at such a comparatively early age, the time-scale for coupling the star's radiative interior to its outer convective zone must be short. Models that allow a star's outer convective zone to be spun down rapidly by wind losses at the 50–100 Myr ages of clusters such as the Pleiades, retaining a hidden reservoir of angular momentum in a rapidly spinning radiative interior, do not show this convergence (Li & Collier Cameron 1993; Krishnamurthi et al. 1997; Allain 1998).

For the core and envelope to be decoupled at the age of the Pleiades but to be rotating synchronously by the age of the Sun, the coupling time-scale must be no less than  $\sim 10$  Myr and no more than 1 Gyr (Soderblom, Jones & Fischer 2001). Rotational evolutionary tracks with coupling time-scales of order 100 Myr do not converge, because the 'buried' angular momentum re-emerges at ages of a few hundred Myr. The wide range of spin rates seen in the very youngest clusters then re-asserts itself, inducing a large scatter in the predicted rotation rates and delaying convergence well beyond the age of Coma and the Hyades.

The Hyades study by Radick et al. (1987) remained unparalleled for nearly two decades after its publication. The advent of wide-field synoptic surveys for exoplanetary transits in open clusters using 1-m class telescopes, and in nearby field stars using even smaller instruments, has led to a recent resurgence of interest in the rotation distributions of open clusters with ages of  $\sim 150$  Myr and older. Several recent photometric studies show the convergence of spin rates in nearby open clusters of intermediate age, notably M35 (150 Myr; Meibom, Mathieu & Stassun 2009), M34 (250 Myr: Irwin et al. 2006) and M37 (550 Myr: Messina et al. 2008; Hartman et al. 2009). These studies have gained new significance because the rotation-age-colour relations in these clusters provide important calibration points for stellar rotational evolution. An empirical calibration of stellar spin rates as a function of age and colour was published recently by Barnes (2007), who coined the term *gyrochronology* to describe the inverse process of inferring a star's age from its rotation period and colour. If magnetic braking causes stellar spin rates to converge by the age of the Hyades (or perhaps sooner) and subsequently to spin-down as some unique and measurable function of time, gyrochronology becomes very attractive as a clock for measuring the ages of individual field stars, stellar and planetary systems.

While this convergence of spin rates seems to be essentially complete among F and G stars by the age of M35 (Meibom et al. 2009), and in K stars by the age of the Hyades, it takes even longer for stars of still lower mass. Although many stars with  $B - V > 1.3$  have converged to the main period-colour relation by the 550 Myr age of M37, Hartman et al. (2009) identified a substantial clump of stars redder than this limit having periods of 2.5 days or less. In their preliminary investigation of the still older Praesepe (650 Myr), Scholz & Eislöffel (2007) find convergence to be completed down to the late K types, but rapid rotation persisting among low-mass stars of spectral type M0 and later.

Here, we present the results of a wide-field photometric monitoring survey of stars brighter than  $V = 14$  in the region around the Coma Berenices open cluster, using the SuperWASP camera array on La Palma. This cluster, also known as Melotte 111, is centred at RA =  $12^{\text{h}}23^{\text{m}}$ , Dec. =  $+26^{\circ}00$  (J2000.0). It is the second closest open cluster to the Sun, lying at a distance of  $89.9 \pm 2.1$  pc (van Leeuwen 1999), further only than the Hyades (46.3 pc: Perryman et al. 1997). The foreground reddening is  $E(B - V) \simeq 0.006 \pm 0.013$  (Nicolet 1981). Trumpler (1938) used proper-motion, radial velocity and colour-magnitude (CM) selection criteria to identify 37 probable members with photographic magnitudes  $m_{\text{pg}} < 10.5$  within  $3.5^{\circ}$  of the cluster centre. Fainter candidates with  $m_{\text{pg}} < 15.0$  were identified within the same region in a proper motion survey by Artiukhina (1955), but only two of these were confirmed by Argue & Kenworthy (1969), who identified another two faint objects that were later confirmed as members. Odenkirchen, Soubiran & Colin (1998) performed a thorough kinematic and photometric survey down to  $V \simeq 10.5$  using the *Hipparcos* and the combined Astrometric Catalogue and TYCHO (ACT; Urban, Corbin & Wycoff 1998) reference catalogues. This study yielded around 50 probable kinematic members in a region of  $1200 \text{ deg}^2$  about the cluster centre, effectively superseding the kinematic and photometric aspects of Trumpler's original survey. Casewell, Jameson & Dobbie (2006) compiled a list of previously known members (according to proper-motion, photometric and in some cases radial velocity criteria) within  $4^{\circ}$  of the cluster centre. They found a further 60 candidate cluster members using the United States Naval Observatory (USNO) B1.0 (Monet et al. 2003) and Two-Micron All-Sky Survey (2MASS) point-source catalogues to carry out proper motion and photometric surveys, respectively, more than doubling the number of probable Melotte 111 cluster members to about 110 according to photometric and kinematic criteria. Among these, about 40 are secure in the sense that they also satisfy radial velocity membership criteria, at least at the level of precision achieved by Trumpler (1938).

Previous photometric studies by Radick, Skiff & Lockwood (1990) of four early-G dwarfs and by Marilli, Catalano & Frasca (1997) of three late-G dwarfs in the Coma Berenices cluster suggest a Hyades-like convergence in spin rates. Like the Hyades, however, Coma Berenices is a difficult target for high-precision photometric rotation studies, because of its age and its wide angular extent. As in the Hyades, the stellar spin periods are expected to range from 6 days among late-F dwarfs to 14 days among mid-K dwarfs, with more rapid rotation persisting at later spectral types. Although stellar dynamos still produce strong magnetic activity signatures at such rotation rates, the starspot coverage is substantially lower than in the ultrafast rotators found in younger open clusters. The comparatively low starspot coverage on stars in the Hyades and Coma yields amplitudes of rotational modulation of at most 1 or 2 per cent. This combination of long periods, low amplitudes and large angular separation between cluster members presents a challenge to observers seeking precise measurements of their optical modulation periods.

In Sections 2 and 3, we describe the observations and data reduction methodology. In Section 4, we describe the generalized Lomb-Scargle period-search method we used to identify candidate rotational variable stars in the Coma Berenices region, while in Section 5 we describe the additional photometric and astrometric criteria used to assess their cluster membership probabilities. In Sections 6 and 7, we discuss the period-colour relation for Coma Berenices cluster members, and the implications for stellar spin-down and gyrochronological age determination.

**Table 1.** Journal of SuperWASP observations for the Coma Berenices rotation survey.

Field centre hhmm+ddmm	No of images	Usable nights	Start date	Baseline (nights)
1143+3126	1200	51	2/5/04	78
1144+2427	1203	52	2/5/04	78
1216+3126	1111	51	2/5/04	78
1217+2326	1200	51	2/5/04	78
1243+3126	2378	86	2/5/04	103
1244+2427	2383	86	2/5/04	103
1217+2350	4876	71	30/12/06	137
1222+3000	4926	72	30/12/06	137
1238+3135	5815	78	14/1/07	137
1241+3924	5796	77	14/1/07	137
1242+2418	5667	76	14/1/07	137
1252+1735	5707	77	14/1/07	137

## 2 OBSERVATIONS

The SuperWASP camera array, located at the Observatorio del Roque de los Muchachos on La Palma, Canary Islands, carried out its inaugural season of observations during 2004. The camera array is mounted on a robotic equatorial mount. In 2004, it comprised five 200-mm f/1.8 Canon lenses each with an Andor CCD array of  $2048^2$   $13.5 \mu\text{m}$  pixels, giving a field of view  $7.8 \text{ deg}^2$  for each camera (Pollacco et al. 2006). Four individual camera, fields covering the region around the Coma Cluster were observed on 51 nights of good photometric quality between 2004 May 2 and 2004 July 18; further two fields at an adjacent pointing position were observed on 86 nights between 2004 May 02 and 2004 August 12.

The Coma Berenices region was re-observed throughout the first half of 2007. By this time, a further three cameras had been installed on the mount. Again, six individual camera fields provided full coverage of the region around the cluster: two on 72 nights from 2006 December 12 to 2007 May 15 and four from 2007 January 14 to May 30.

The survey region was accessible for between 4 and 8 h each night. The average interval between visits to the field was 6 min. Each exposure was of 30 s duration, and was taken without filters in 2004, and with an infrared blocking filter in 2007.

The field centres and dates of observation are summarized in Table 1.

## 3 DATA REDUCTION AND CALIBRATION

The data were reduced using the SuperWASP data reduction pipeline, whose operation is described in detail by (Pollacco et al. 2006). Science frames are bias-subtracted and flat-fielded. An automated field recognition algorithm identifies the objects on the frame with their counterparts in the TYCHO-2 catalogue and establishes an astrometric solution with an rms precision of 0.1–0.2 pixel. The pipeline then performs aperture photometry at the positions on each CCD image of all objects in the USNO-B1.0 catalogue (Monet et al. 2003) with magnitudes in the  $R2$  band brighter than 14.5, equivalent to  $V \simeq 15$  over the colour range  $0 < B - V < 1$ . The pipeline computes the formal variance of the flux of each star in the image from the photon counts in the stellar aperture and the surrounding sky annulus. This magnitude limit is dictated by the detection threshold for the SuperWASP exoplanetary transit-search project; stars with  $R2 \simeq 14.5$  yield light curves with rms scatter between 0.02 and 0.03 mag.

The SuperWASP bandpass covers most of the optical spectrum, so the effective atmospheric extinction depends on stellar colour. The extinction correction to zero airmass for a star of known  $B - V$  colour index takes the form

$$m_0 = m - k'X - k''(B - V)X,$$

where  $m$  is the raw instrumental magnitude at airmass  $X$ ,  $m_0$  is the instrumental magnitude above the atmosphere and  $k'$  and  $k''$  are the primary and secondary extinction coefficients, respectively. The zero-point  $z$  for each image is tied to a network of local secondary standards in each field. The resulting instrumental magnitudes are transformed to TYCHO-2 $V$  magnitudes via the colour equation

$$V_T = m_0 - z - c(B - V),$$

where the colour transformation coefficient for all cameras lies in the range  $c = -0.22 \pm 0.03$ . The resulting fluxes are stored in the SuperWASP Data Archive at the University of Leicester.

We extracted the light curves of all stars observed in the six fields nearest to the centre of the Coma cluster in each of the 2004 and 2007 observing seasons from the archive. We stored them in a two-dimensional array whose columns held the light curves of individual stars, and whose rows held data derived from individual CCD frames. Patterns of correlated systematic error were identified and removed using the SYSREM algorithm of Tamuz, Mazeh & Zucker (2005), as implemented by Collier Cameron et al. (2006). At this stage, the photometric variances are augmented by an additional systematic variance that accounts for the actual scatter in the measured fluxes about the final decorrelated solution for each frame. The maximum-likelihood algorithm for computing this additional variance is described by Collier Cameron et al. (2006). The long-term rms scatter of the decorrelated SuperWASP light curve of a non-variable star is 0.004 mag at  $V = 9.5$ , degrading to 0.01 mag at  $V = 12.0$  as shown in fig. 3 of Collier Cameron et al. (2006).

## 4 LIGHT CURVE ANALYSIS

### 4.1 Frequency analysis

We searched for evidence of quasi-sinusoidal light curve modulation in all stars in the field, using the generalized Lomb–Scargle periodogram formulation of Zechmeister & Kürster (2009) to fit an inverse variance-weighted floating mean sinusoid to the light curve over a full observing season.

Each star's light curve comprises a set of observed magnitudes  $m'_i \in \{m'_1, m'_2, \dots, m'_N\}$  with associated variances  $\sigma_i^2 \in \{\sigma_1^2, \sigma_2^2, \dots, \sigma_N^2\}$ . We form differential magnitudes

$$m_i = m'_i - \hat{m},$$

where

$$\hat{m} = \frac{\sum_i m'_i / \sigma_i^2}{\sum_i 1 / \sigma_i^2}.$$

The goodness of fit of this constant-magnitude model to the light curve is given by the statistic

$$\chi_0^2 = \sum (m_i)^2 / \sigma_i^2.$$

We fit a sinusoidal model

$$y_i = A \cos \omega t_i + B \sin \omega t_i + C$$

with angular frequency  $\omega$  to the residuals  $m_i$  at the times  $t_i$  of observation. We solve for the coefficients  $A$ ,  $B$  and  $C$  using the algorithms

of Zechmeister & Kürster (2009). The light curve amplitude at frequency  $\omega$  is then

$$\delta m = \sqrt{\hat{A}^2 + \hat{B}^2}$$

and its associated variance is

$$\text{Var}(\delta m) = \frac{\hat{A}^2 \text{Var}(\hat{A}) + \hat{B}^2 \text{Var}(\hat{B})}{\hat{A}^2 + \hat{B}^2}.$$

We repeat the process at a set of frequencies corresponding to periods ranging from 1.11 to 20 days. At each frequency  $\omega$ , we compute the statistic

$$p(\omega) = \frac{\chi_0^2 - \chi^2(\omega)}{\chi_0^2}.$$

For each star, the peak value  $p_{\text{best}}$  of the  $p$  statistic is achieved at the frequency at which  $\chi^2$  is minimized.

For a light curve comprising  $N$  independent measurements, Cumming, Marcy & Butler (1999) estimate

$$\text{Prob}(p > p_{\text{best}}) = (1 - p_{\text{best}})^{(N-3)/2}. \quad (1)$$

The false-alarm probability (FAP) for  $M$  independent frequency measurements is then

$$\text{FAP} = 1 - [\text{Prob}(p > p_{\text{best}})]^M, \quad (2)$$

where  $M \simeq T(f_2 - f_1)$  for a data train of total duration  $T$  searched in the frequency range  $f_1 < f < f_2$  (Cumming 2004).

The FAP is sensitive to the number  $N$  of independent observations. As Collier Cameron et al. (2006) found, some forms of correlated error repeat at intervals of 1 day, and are not adequately removed by the SYSREM algorithm. A small misalignment of SuperWASP's polar axis causes every stellar image to drift across the frame by a few tens of pixels during each night. The vignetting pattern of the camera lenses produces discontinuities in the focal-plane illumination gradient near the edge of the frame, which change slightly from night to night and even during the course of a single night. The resulting correlated errors serve to reduce the number of independent observations from  $N$  to a lower value  $N_{\text{eff}}$ .

We estimated  $N_{\text{eff}}$  by randomizing the order of the list of dates on which data were obtained. The shuffling procedure shifts each night's observations in their entirety to a new date. This procedure effectively destroys coherent signals with periods longer than 1 day, but retains the global form of the window function and the effects of correlated noise. If many such trials are made, we expect  $p_{\text{best}}$  in their individual periodograms to exceed the value found for a single randomly chosen trial roughly half the time. We thus estimate a false-alarm probability  $\text{FAP}_0 = 0.5$  for the strongest peak  $p_{\text{best}}$  in the periodogram of the shuffled data. Using this estimate, we combine and invert equations (1) and (2) to obtain an estimate of the effective number of independent observations in the presence of correlated errors:

$$N_{\text{eff}} \simeq \frac{3 \ln(1 - p_{\text{best}}) + 2 \ln[1 - (1 - \text{FAP}_0)^{1/M}]}{\ln(1 - p_{\text{best}})}. \quad (3)$$

In practice, we found that typically  $N_{\text{eff}} \simeq N/10$ . Since SuperWASP observes each field at intervals of 8 min or so, the effective correlation time is of the order of 1.5 h.

In Fig. 1, we plot the best-fitting modulation amplitude against FAP for all stars in the field SW1216+3126 observed in the 2004 season. We select for further study all those light curves showing evidence of periodic modulation with FAPs less than  $10^{-2}$ . These stars exhibit light curve amplitudes in the range 0.01–0.1 mag, which is typical of rotational variables with periods of the order of a few days.

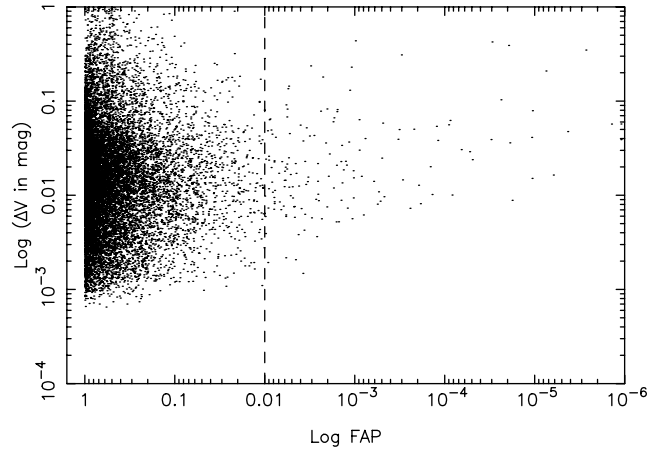


**Figure 1.** Amplitude of best-fitting sinusoidal model as a function of FAP for stars in the field SW1216+3126 in the 2004 season. Stars to the right of the selection threshold set at  $\text{FAP} = 10^{-2}$  are considered to be candidate rotational variables.

## 5 CANDIDATE SELECTION

Having identified a large number ( $N_{\text{tot}} = 1613$ ) of rotational variables in the vicinity of the cluster, the next step is to determine which among them are likely to be cluster members. We followed the method of Girard et al. (1989), defining probability density functions for the proper motions of  $N_c$  cluster members and  $N_f = N_{\text{tot}} - N_c$  field stars.

We obtained proper motions and magnitudes in the  $V$  and 2MASS  $J$  and  $K_s$  bands for all candidate rotational variables by cross-matching with the Naval Observatory Merged Astrometric Dataset (NOMAD) catalogue (Zacharias et al. 2005). Following Casewell et al. (2006), we adopt  $\mu_\alpha = -11.21 \pm 0.26 \text{ mas yr}^{-1}$  and  $\mu_\delta = -9.16 \pm 0.15 \text{ mas yr}^{-1}$  as the mean proper motion of the known cluster members, as determined by van Leeuwen (1999). The proper-motion diagram for the full sample is shown in Fig. 2. The field distribution for stars with total proper motions less than  $25 \text{ mas yr}^{-1}$  is approximated by a two-dimensional gaussian

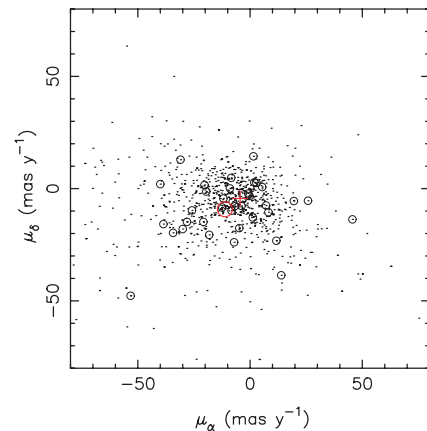


**Figure 2.** Proper-motion diagram of stars with significant ( $\text{FAP} < 10^{-2}$ ) quasi-sinusoidal variability and periods between 1.1 and 20 days, in the WASP fields surveyed in 2004 and 2007. The red cross denotes the centroid of the field distribution for stars with total proper motions less than  $25 \text{ mas yr}^{-1}$ , while the red circle marks the mean proper motion of the cluster members. The 30 stars with combined kinematic and photometric membership probabilities greater than 0.5 (see also Table 2) are encircled.

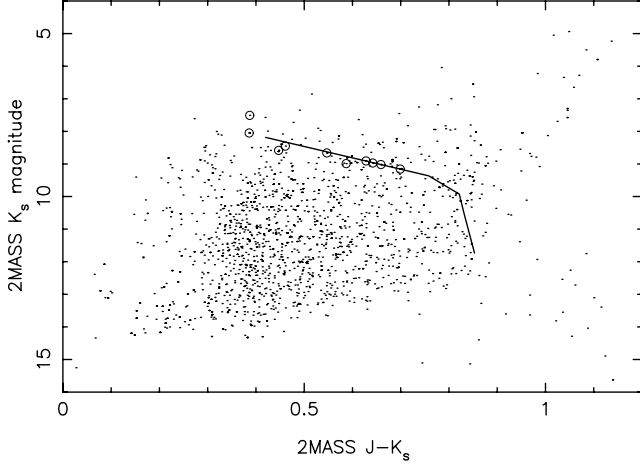


**Figure 3.** 2MASS ( $K$ ,  $J - K$ ) CM diagram of stars with significant ( $\text{FAP} < 10^{-2}$ ) quasi-sinusoidal variability and periods between 1.1 and 20 days, in the WASP fields surveyed in 2004 and 2007. Previously known cluster members detected as rotational variables and satisfying our cluster membership criteria are encircled. The solid curve is the 520 Myr isochrone of Baraffe et al. (1998) for stars of solar metallicity at the distance of the Coma Berenices cluster.

probability density function having the form

$$f_f = \frac{N_f}{2\pi\Sigma_{f\alpha}\Sigma_{f\delta}} \exp\left[-\frac{(\mu_{\alpha i} - \mu_{f\alpha})^2}{2\Sigma_{f\alpha}^2} - \frac{(\mu_{\delta i} - \mu_{f\delta})^2}{2\Sigma_{f\delta}^2}\right], \quad (4)$$

with mean proper motion  $\mu_{f\alpha} = -4.42 \text{ mas yr}^{-1}$ ,  $\mu_{f\delta} = -4.39 \text{ mas yr}^{-1}$  and dispersion  $\Sigma_{f\alpha} = 9.90 \text{ mas yr}^{-1}$ ,  $\Sigma_{f\delta} = 8.18 \text{ mas yr}^{-1}$ .

For cluster members, the density function depends primarily on the uncertainties in the proper-motion components  $\sigma_{\alpha i}$  and  $\sigma_{\delta i}$  for the individual stars, since the intrinsic spread in the proper motions of the cluster members is smaller than the measurement errors:

$$f_c = \frac{N_c}{2\pi\sigma_{c\alpha}\sigma_{c\delta}} \exp\left[-\frac{(\mu_{\alpha i} - \mu_{c\alpha})^2}{2\sigma_{\alpha i}^2} - \frac{(\mu_{\delta i} - \mu_{c\delta})^2}{2\sigma_{\delta i}^2}\right]. \quad (5)$$

Following Girard et al. (1989), the cluster membership probability for an individual star is

$$p = \frac{f_c}{f_c + f_f}.$$

We generalized this approach to take into account the magnitude distribution of field stars and proximity to the cluster main sequence in a CM diagram constructed from the 2MASS  $K$  magnitudes and  $J - K$  colour index (Fig. 3). To select likely cluster members using their locations in this CM diagram, we adopted the 520 Myr isochrone from Baraffe's (1998) NEXTGEN stellar evolution models, for low-mass stars of solar metallicity. The theoretical absolute  $K$  magnitudes were converted to apparent magnitudes using the *Hipparcos* distance of  $89.9 \pm 2.1 \text{ pc}$  to the cluster (van Leeuwen 1999). The Baraffe  $J - K$  colour and  $K$  magnitude were converted from the Caltech (CIT) system for which they were computed to their 2MASS equivalents using the transformation of Carpenter (2001). We allow an intrinsic scatter  $\Sigma_{cK} = 0.15 \text{ mag}$  about the theoretical main sequence, assuming the depth of the cluster to be of the order of the 5–6 pc tidal radius estimated by Odenkirchen et al. (1998). The probability density function is assumed to be gaussian.

Because the SuperWASP bandpass is in the optical range, the CM diagram of the field stars shows  $K_s$  magnitude to be correlated

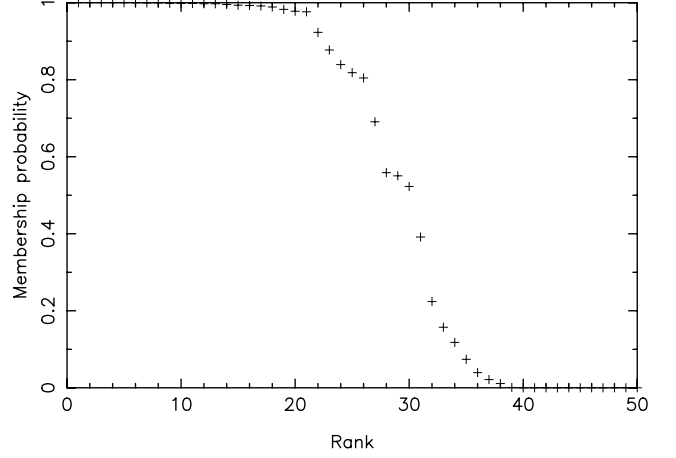


**Figure 4.** Ranked cluster membership probabilities of the top 50 stars (+) whose light curves recorded by one or more WASP cameras in 2004 or 2007 showed significant ( $\text{FAP} < 10^{-2}$ ) quasi-sinusoidal variability and periods between 1.1 and 20 days. The membership probability is determined from the proper motions and  $K$  magnitude distributions for cluster and field stars, as described in the text. 30 stars have cluster membership probabilities greater than 0.5.

with  $J - K$  colour. The offset in  $K$  magnitude of a star  $i$  from the mean relation is given by

$$\delta K_{fi} = K_i - 11.700 + 2.808((J - K)_i - 0.461)$$

with an approximately gaussian intrinsic scatter  $\Sigma_{fK} = 1.38 \text{ mag}$ .

We multiply the probability densities for the  $K_s$  magnitude offset from the field distributions with the field proper-motion probability density from equation (4) above to obtain

$$g_f = \frac{f_f}{\sqrt{2\pi}\Sigma_{fK}} \exp\left(-\frac{\delta K_{fi}^2}{\Sigma_{fK}^2}\right), \quad (6)$$

and similarly for the cluster probability density we obtain

$$g_c = \frac{f_c}{\sqrt{2\pi}\Sigma_{cK}} \exp\left[-\frac{(K_i - K_{\text{isochrone}})^2}{\Sigma_{cK}^2}\right]. \quad (7)$$

The combined membership probability for an individual star is then

$$p = \frac{g_c}{g_c + g_f}.$$

In Fig. 4, we plot the cluster membership probabilities of the 50 rotational variables that are the most likely cluster members, in descending order of rank. The properties of the 30 stars with membership probabilities greater than 0.5 are listed in Table 2, together with cross-identifications with previous catalogues of cluster members.

## 6 PERIOD-COLOUR RELATION

The rotation periods of all stars with FAPs less than 0.01 and membership probabilities greater than 0.5 are plotted as a function of  $J - K$  colour in Fig. 5. Among these, the periods of stars with cluster membership probabilities greater than 0.85 are denoted by solid symbols. They follow a tight period–colour relation. The properties of these stars are listed in Table 2, including cross-identifications with previous catalogues of cluster members. The rotational parameters of individual light curves that yielded significant detections in the 2004 and 2007 seasons are listed in Table 3.

Several light curves yield periods that follow a second sequence in Fig. 5, with periods close to half those on the main relation.

**Table 2.** Cross-identifications, 2MASS photometry and proper motions of candidate rotational variables with membership probabilities greater than 0.5.

1SWASP	USNO B-1.0	Cl Melotte 111	Spectral type	$J - K$	$K_s$	$\theta$ ( $^\circ$ )	$\mu_\alpha$ (mas yr $^{-1}$ )	$\mu_\delta$ (mas yr $^{-1}$ )	Membership probability
J114837.70+281630.5	1182-0217523	New member	G8	0.430	8.585	7.976	$-10.6 \pm 0.7$	$-7.6 \pm 0.7$	0.976 465
J115533.35+294341.7	1197-0194906	New member	K3	0.635	9.057	7.117	$-7.9 \pm 0.9$	$-8.2 \pm 1.1$	0.993 480
J120052.24+271923.9	1173-0240221	New member	K4	0.678	8.996	5.118	$-11.9 \pm 0.7$	$-4.4 \pm 0.7$	0.997 313
J120222.86+225458.7	1129-0233236	New member	K4	0.787	9.603	5.614	$-4.3 \pm 1.3$	$2.9 \pm 1.1$	0.818 328
J120757.72+253511.3	1155-0190903	AV 189	K3	0.628	8.906	3.410	$-11.5 \pm 1.2$	$-7.7 \pm 0.9$	0.998 392
J120836.10+310609.9	1211-0194040	New member	K7	0.765	9.402	6.002	$-16.8 \pm 1.6$	$-4.1 \pm 2.0$	0.977 817
J121135.15+292244.5	1193-0195921	New member	K4	0.596	8.979	4.219	$-12.5 \pm 0.8$	$-9.9 \pm 0.9$	0.997 246
J121253.23+261501.3	1162-0201218	AV 523	K2	0.587	8.990	2.284	$-11.0 \pm 1.1$	$-9.0 \pm 0.7$	0.991 622
J122115.62+260914.0	1161-0200668	AV 1183	K4	0.642	8.972	0.420	$-13.1 \pm 1.4$	$-9.2 \pm 1.0$	0.998 253
J122347.22+231444.3	1132-0216856	AV 1404	K4	0.659	9.018	2.760	$-12.5 \pm 0.6$	$-8.4 \pm 0.6$	0.999 326
J122601.31+342108.4	1243-0197448	New member	K5	0.702	9.143	8.378	$-2.1 \pm 1.8$	$-5.4 \pm 2.2$	0.922 972
J122651.03+261601.8	1162-0204591	AV 1660	K4	0.699	9.156	0.905	$-13.3 \pm 1.3$	$-4.4 \pm 1.1$	0.992 839
J122720.68+231947.4	1133-0208375	AV 1693	G8	0.461	8.451	2.847	$-11.5 \pm 0.7$	$-8.8 \pm 0.6$	0.999 931
J122748.29+281139.8	1181-0230534	AV 1737, T141	G8	0.386	8.050	2.441	$-13.1 \pm 0.6$	$-8.7 \pm 0.6$	0.999 997
J122856.43+263257.4	1165-0203085	AV 1826, T220	K1	0.547	8.661	1.441	$-12.6 \pm 0.7$	$-9.2 \pm 0.8$	0.999 831
J123231.07+351952.2	1253-0200298	New member	G0	0.321	8.086	9.552	$-12.2 \pm 1.4$	$-10.7 \pm 1.0$	0.999 935
J123320.01+222423.3	1124-0241610	New member	G8	0.453	8.402	4.297	$-12.6 \pm 0.7$	$-8.5 \pm 0.7$	0.999 955
J123342.12+255634.0	1159-0194918	AV 2177	K0	0.447	8.584	2.406	$-10.7 \pm 0.7$	$-7.7 \pm 0.7$	0.995 428
J123454.29+272720.2	1174-0253286	AV 2257	G0	0.387	7.510	3.031	$-9.8 \pm 1.2$	$-8.9 \pm 0.6$	0.550 545
J123811.47+233322.2	1135-0193392	New member	M0	0.813	9.963	4.226	$-12.0 \pm 5.8$	$-8.6 \pm 5.8$	0.522 927
J123941.99+213458.0	1115-0215169	New member	K5	0.689	8.799	5.839	$-6.6 \pm 0.7$	$-3.5 \pm 1.7$	0.558 604
J124235.14+410527.7	1310-0230997	New member	K5	0.683	9.273	15.626	$-7.1 \pm 1.5$	$-1.4 \pm 2.1$	0.804 599
J124900.42+252135.6	1153-0197249	New member	K5	0.681	9.069	5.894	$-10.3 \pm 0.7$	$-6.8 \pm 0.7$	0.997 940
J124930.43+253211.1	1155-0197399	New member?	K5	0.682	8.931	5.985	$-15.3 \pm 1.4$	$-6.0 \pm 2.1$	0.982 752
J125001.70+210312.1	1110-0214013	New member	K3	0.582	8.976	7.925	$-13.4 \pm 1.4$	$8.1 \pm 1.5$	0.839 267
J125211.61+252224.5	1153-0197624	New member	F8	0.272	7.609	6.606	$-12.8 \pm 1.2$	$-9.0 \pm 1.0$	1.000 000
J125314.67+240313.6	1140-0196476	New member	K5	0.750	9.452	7.121	$5.3 \pm 2.7$	$-17.1 \pm 3.9$	0.690 814
J125736.86+285844.7	1189-0206667	New member	G8	0.424	8.473	8.231	$-12.5 \pm 0.6$	$-7.5 \pm 0.7$	0.999 222
J125927.75+194115.1	1096-0208690	New member	K5	0.692	9.034	10.502	$-9.3 \pm 5.3$	$-9.7 \pm 5.5$	0.877 254
J130543.99+200321.4	1100-0213302	New member	K2	0.605	8.922	11.481	$3.5 \pm 0.6$	$-6.4 \pm 1.0$	0.989 022

*Note.* The 1SWASP identifier encodes the J2000.0 coordinates of the object.  $\theta$  denotes the angular distance of the star from the cluster centre. The spectral types are estimated from 2MASS photometry using the calibration of Blackwell & Lynas-Gray (1994).

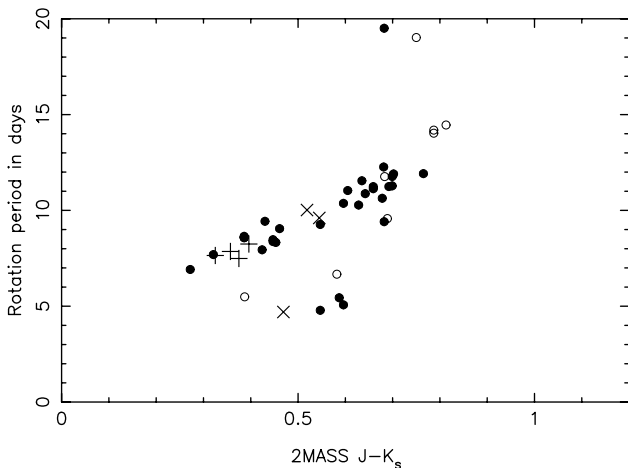


**Figure 5.** Photometric rotation period as a function of 2MASS ( $J - K$ ) colour for stars with significant ( $FAP < 10^{-2}$ ) quasi-sinusoidal variability and cluster membership probability greater than 0.5, in the WASP fields surveyed in 2004 and 2007. Periods measured for candidates with cluster membership probabilities greater than 0.85 are denoted by filled circles; those with membership probabilities between 0.5 and 0.85 are denoted by open circles. Additional stars from Radick et al. (1990) and Marilli et al. (1997) are denoted by ‘+’ and ‘x’ symbols, respectively.

A similar secondary period–colour sequence was noted by Hartman et al. (2009) in their recent study of the comparably aged cluster M37. Several of them were recorded independently in two or more of the WASP cameras, and some in different seasons, and were found to jump between the two relations. The K4 dwarf 1SWASP J121135.15+292244.5, for example, yields  $P = 10.37$  d in 2004 and 5.07 d in 2007. Similarly, the K1 dwarf J122856.43+263257.4 yielded periods of 4.79 d in 2004 and 9.26d in 2007. The K2 dwarf 1SWASP J121253.23+261501.2 yields 10.38 d in 2004 and 5.44 d in 2007, though only the latter measurement has  $FAP < 0.01$  and is listed here.

These stars almost certainly rotate with periods near the main relation. The reason for the intermittent frequency doubling is apparent from Fig. 6. The 2004 light curve yields a period half that of the 2007 light curve, but the longer period is clearly present in both seasons. Evidently, the apparent doubling of these stars’ rotational frequencies at some epochs of observation arises from two dominant starspot groups on opposing stellar hemispheres giving a double-humped light curve. We conclude that the true periods of the light curves on the lower sequence are twice those derived from sine fitting. After correcting for frequency doubling, the period–colour relation is as shown in Fig. 7.

Among the stars with membership probabilities greater than 0.85, only one outlier is seen with a period that departs significantly

**Table 3.** Sine-fitting periods for light curves of candidate rotational variables in the vicinity of Melotte 111, with cluster membership probabilities greater than 0.5.

ISWASP	Season	Field_cam	Nobs	Period (days)	Amplitude (mag)	FAP
J114837.70+281630.5	2004	SW1143+3126_102	1138	9.43	0.005	0.000 079
J115533.35+294341.7	2004	SW1143+3126_102	1139	11.55	0.005	0.001 371
J120052.24+271923.9	2007	SW1217+2350_142	2841	10.63	0.010	0.000 374
J120222.86+225458.7	2004	SW1217+2326_104	1149	14.03	0.004	0.007 144
J120222.86+225458.7	2007	SW1217+2350_142	2824	14.19	0.008	0.001 182
J120757.72+253511.3	2007	SW1217+2350_142	2841	10.28	0.005	0.003 890
J120836.10+310609.9	2007	SW1222+3000_144	2960	11.92	0.007	0.002 868
J121135.15+292244.5	2004	SW1216+3126_103	1034	10.37	0.009	0.001 038
J121135.15+292244.5	2007	SW1222+3000_144	2959	(5.07)	0.006	0.001 124
J121253.23+261501.3	2007	SW1217+2350_142	2840	(5.44)	0.006	0.006 021
J122115.62+260914.0	2004	SW1217+2326_104	1147	10.88	0.011	0.000 146
J122347.22+231444.3	2004	SW1217+2326_104	1149	11.13	0.010	0.003 327
J122347.22+231444.3	2007	SW1217+2350_142	2841	11.24	0.009	0.000 749
J122601.31+342108.4	2004	SW1216+3126_103	1034	11.90	0.023	0.001 428
J122651.03+261601.8	2004	SW1244+2427_101	2269	11.77	0.005	0.000 632
J122651.03+261601.8	2007	SW1222+3000_144	2910	11.28	0.006	0.008 509
J122656.48+224054.7	2004	SW1244+2427_101	2265	(5.77)	0.020	0.006 039
J122720.68+231947.4	2004	SW1244+2427_101	2183	9.05	0.006	0.000 308
J122748.29+281139.8	2007	SW1222+3000_144	2904	8.65	0.010	0.002 253
J122748.29+281139.8	2007	SW1238+3135_143	3255	8.57	0.012	0.000 008
J122748.29+281139.8	2007	SW1242+2418_141	3575	8.59	0.011	0.000 008
J122856.43+263257.4	2004	SW1244+2427_101	2268	(4.79)	0.006	0.001 287
J122856.43+263257.4	2007	SW1242+2418_141	3833	9.26	0.007	0.006 194
J122942.15+283714.6	2007	SW1222+3000_144	2894	16.05	0.004	0.003 018
J123231.07+351952.2	2004	SW1243+3126_102	2259	7.69	0.008	0.000 009
J123320.01+222423.3	2007	SW1242+2418_141	3833	8.33	0.006	0.001 505
J123341.88+291401.7	2007	SW1222+3000_144	2790	16.88	0.010	0.006 104
J123342.12+255634.0	2004	SW1217+2326_104	1147	8.38	0.010	0.003 695
J123342.12+255634.0	2007	SW1242+2418_141	3831	8.47	0.009	0.000 000
J123354.22+270804.7	2007	SW1222+3000_144	2722	16.54	0.008	0.006 181
J123454.29+272720.2	2004	SW1216+3126_103	1017	(5.49)	0.013	0.004 207
J123811.47+233322.2	2007	SW1242+2418_141	3828	14.46	0.013	0.000 240
J123941.99+213458.0	2004	SW1244+2427_101	2264	9.57	0.004	0.007 075
J124235.14+410527.7	2007	SW1241+3924_148	3548	11.76	0.003	0.003 510
J124309.53+244705.2	2007	SW1242+2418_141	3830	2.77	0.015	0.000 027
J124523.35+425104.4	2007	SW1241+3924_148	3542	12.05	0.030	0.002 383
J124900.42+252135.6	2007	SW1242+2418_141	3822	12.27	0.009	0.000 001
J124930.43+253211.1	2004	SW1244+2427_101	2264	19.51	0.017	0.000 018
J124930.43+253211.1	2007	SW1242+2418_141	3820	(9.41)	0.019	0.000 082
J125001.70+210312.1	2004	SW1244+2427_101	2267	(6.67)	0.003	0.003 746
J125211.61+252224.5	2007	SW1242+2418_141	3815	6.92	0.005	0.007 111
J125314.67+240313.6	2004	SW1244+2427_101	2267	19.02	0.027	0.000 555
J125419.08+324935.1	2004	SW1243+3126_102	2291	15.69	0.003	0.002 814
J125736.86+285844.7	2004	SW1243+3126_102	2279	7.94	0.007	0.003 388
J125927.75+194115.1	2007	SW1252+1735_147	3788	11.24	0.025	0.000 021
J130543.99+200321.4	2007	SW1252+1735_147	3625	11.04	0.003	0.002 140

*Note.* The year of observation is listed, with a designator incorporating the RA and Dec. of the field centre and a three-digit camera identifier for each light curve. The number  $N_{\text{obs}}$  of observations is listed, followed by the period of the peak in the periodogram yielding the greatest improvement in the  $\chi^2$  statistic. Columns 6 and 7 give the amplitude of the fitted sinusoid and the FAP of the signal detection. Periods suspected of being half the true period appear in parentheses.

from the main relation. This star, ISWASP J124930.43+253211.1 ( $J - K = 0.682$ ), exhibited a clear period of 19.51d in 2004, with a weak secondary minimum. In 2007, the period appears to be 9.41 d, but the minima alternate in depth indicating the true period to be 18.82 d. Meibom et al. (2009) noted the presence of several similarly anomalous slow rotators in their rotation study of M35, and proposed that partial or complete tidal synchronization in stellar binary systems could be responsible. Radial velocity observations of this star would be desirable to check

whether it really belongs to the cluster, and to test for evidence of binarity.

Half of the 23 rotational variables with membership probabilities greater than 0.85 lie within  $4^{\circ}2$  of the cluster centre, while the other half lie in the periphery of the cluster, between  $4^{\circ}$  and  $11^{\circ}5$  from the cluster centre. Among them, 14 appear to be previously uncatalogued cluster members. Rotational variability thus appears to be a useful method for identifying new members of the cluster and its extended halo.

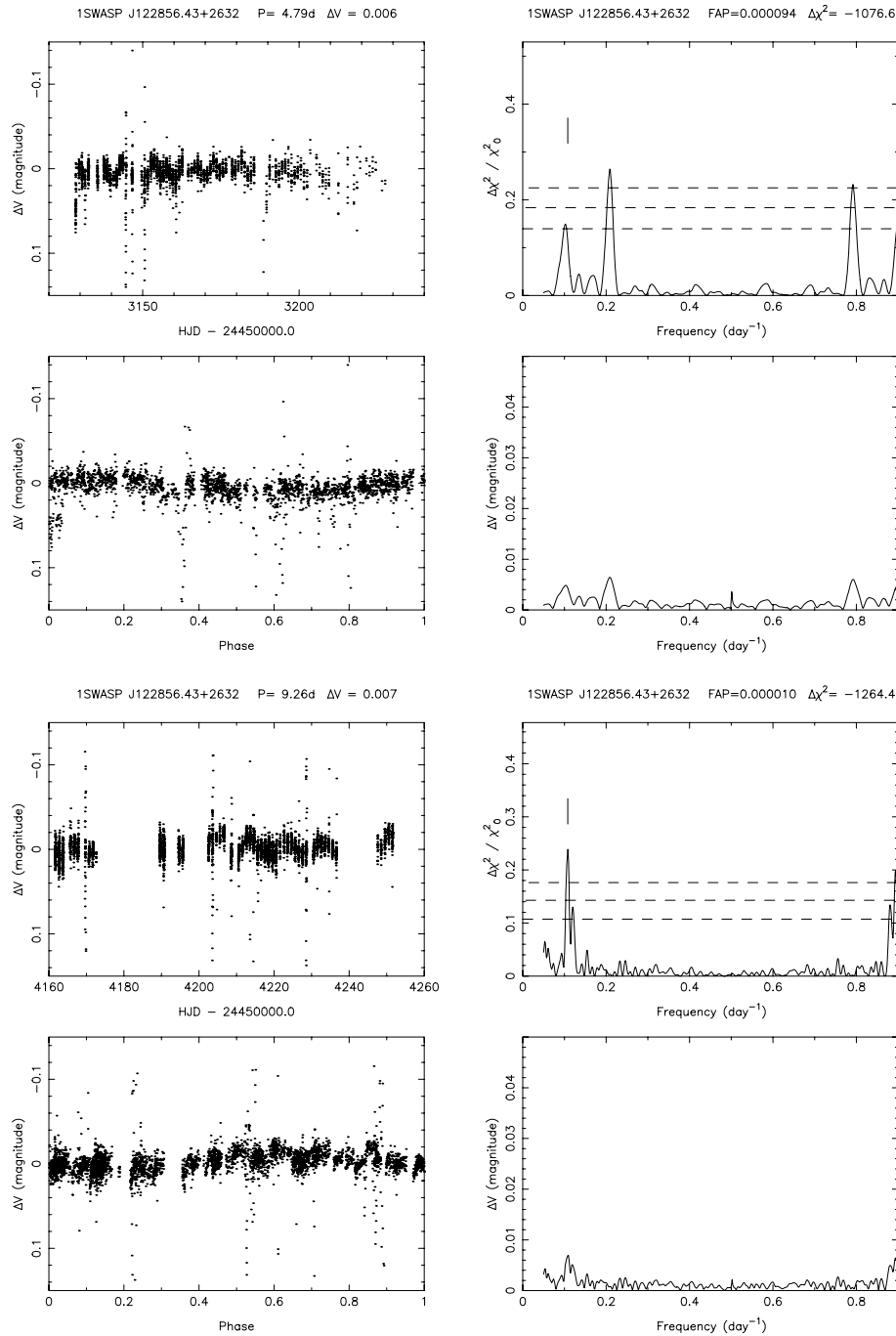


**Figure 6.** Light curves and periodograms for 1SWASP J122856.43+263257.4 observed in 2004 (top) and 2007 (bottom). Each set of four panels shows the unphased light curve at upper left. Occasional gaps in the data were caused by inclement weather. The periodogram of  $p = \Delta\chi^2/\chi_0^2$  versus frequency is at upper right, with horizontal dashed lines denoting thresholds of FAP 0.1, 0.01 and 0.001. The vertical bar indicates the true rotational frequency. The light curve phased on the best-fitting period for the year concerned is shown at lower left, and the sine-wave amplitude periodogram at lower right. The 2004 data illustrate the frequency doubling that occurs when major spot complexes are present on opposite stellar hemispheres, giving a double-humped light curve.

In Figs 5 and 7, we also show previously published photometric periods for Melotte 111 stars T65, T76, T85 and T132 (Radick et al. 1990) and T203, T213 and T221 (Marilli et al. 1997), with their 2MASS colours.

The photometric periods found by Marilli et al. (1997) for T203 and T221 lie close to the SuperWASP period–colour relation. The 4.7-day period they found for T213 is very close to half the period predicted by equation (8). The sine-fitting method reveals a 9.51-

day modulation in the WASP light curve of this star, but the FAP was below the threshold value 0.01 that would qualify it as a secure detection. We adopt a period of 9.4 days for this object, twice that reported by Marilli et al.

Together with the four Radick stars and the three Marilli stars, but excluding the anomalous slow rotator 1SWASP J124930.43+253211.1, the WASP light curves for stars with high cluster-membership probabilities and low FAPs lie along a

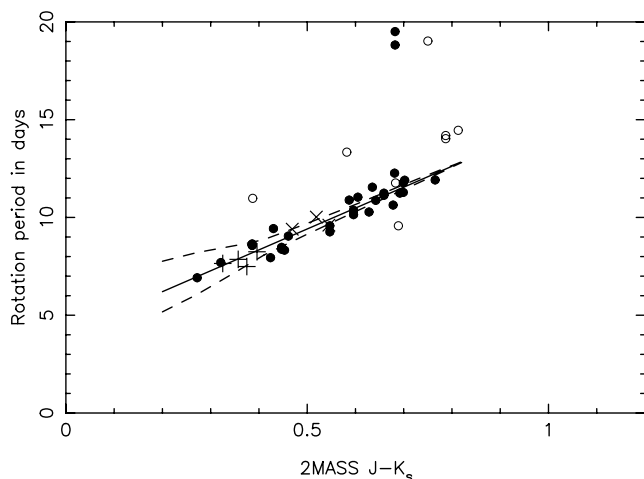


**Figure 7.** As for Fig. 5, with the periods of the light curves on the lower branch having been doubled. The solid line is a least-squares linear fit to the period–colour relation, and the dashed lines delineate the scatter about the mean relation expected from cyclic changes in spot latitude on differentially rotating stars.

well-defined, almost linear period–colour relation. A linear least-squares fit to the period–colour relation of these stars yields

$$P = 9.71 + 10.68(J - K - 0.528). \quad (8)$$

The rms scatter of the observed periods about the fitted period–colour relation is 0.19 days – just 2 per cent of the mean period – and is not improved by the inclusion of quadratic or higher terms. This scatter is so small that much of it is attributable to year-to-year changes in the photometric modulation periods of the cluster stars themselves. There are seven instances in which periods were measured for the same star in both 2004 and 2007. These season-to-season period differences are 0.09, 0.11, 0.16, 0.23, 0.32 and 0.49 days. The season-to-season differences in the period determinations for a given star average 0.23 days, comparable to the scatter about the mean relation. Radick et al. (1995) reported finding very similar season-to-season period variations of between 2 and 8 per cent in their 12-year study of rotation in the Hyades.

There are two possible explanations for this trend: latitudinal differential rotation and core-envelope decoupling, both of whose effects will be superimposed on a spread at all spectral types resulting from a range of disc-locking lifetimes.

Differential rotation on the stars themselves will lead to secular changes in the modulation period, if activity cycles are present which cause the main spot belts to drift in latitude. Doppler imaging and line-profile studies of differential rotation in young main-sequence stars show a strong decrease in latitudinal differential rotation along the main sequence. F and G dwarfs exhibit stronger shear than mid-to-late K dwarfs which rotate almost as solid bodies (Barnes et al. 2005; Reiners 2006). Collier Cameron (2007) gives the empirical relation for the equator-to-pole difference in rotational frequency

$$\Delta\Omega = 0.053(T_{\text{eff}}/5130)^{8.6} \text{ rad d}^{-1}. \quad (9)$$

We expect the resulting scatter in rotation frequency to be no more than half this amount, if the main active belts migrate across a similar range of latitudes as the solar butterfly diagram occupies on the Sun. The corresponding range of rotation periods at each colour is shown in Fig. 7. The dispersions about the main period–colour reported here and by Hartman et al. (2009) in M37 are

comparable to the scatter expected from differential rotation for the F and G stars. The K stars also show season-to-season period changes that are most easily explained by a degree of differential rotation somewhat greater than Doppler imaging studies have found among more rapidly rotating stars of similar mass. At all colours, we find the season-to-season period changes to contribute a significant fraction, though perhaps not all, of the overall scatter about the mean period–colour relation.

Additional residual scatter is expected at all spectral types if the early spin rates of stars are regulated by torque balance with accretion discs having a range of lifetimes. Such ‘disc-locking’ models are reasonably successful at explaining the distribution of stellar spin rates on the zero-age main sequence (Collier Cameron, Campbell & Quaintrell 1995; Keppens, MacGregor & Charbonneau 1995; Krishnamurthi et al. 1997; Allain 1998).

Once the star decouples from the disc, angular momentum is lost through the stellar wind alone, but the spin-down behaviour of the stellar surface depends critically on the degree of coupling between the star’s radiative interior and convective envelope. Stauffer & Hartmann (1987) sought to explain the rapid spin-down of G dwarfs between the ages of the 50 Myr old  $\alpha$  Per cluster and the 70 Myr old Pleiades by suggesting that magnetic braking early in a star’s life may spin-down only the outer convective layers at first, leaving a decoupled reservoir of angular momentum in the stellar radiative core. If the coupling time-scale on which the stored angular momentum is transported from the core back into the envelope is longer than a few tens of Myr, outward angular momentum transport will spin-up the envelope at intermediate ages. This will counter the effects of magnetic braking and delay full convergence to a single period–colour relation. The effect would be lessened in K dwarfs, whose radiative interiors comprise a smaller fraction of the total stellar moment of inertia.

Several authors have modelled and discussed the implications of core-envelope decoupling for cluster period distributions at various ages (Li & Collier Cameron 1993; Collier Cameron & Li 1994; Krishnamurthi et al. 1997; Allain 1998; Wolff, Strom & Hillenbrand 2004; Soderblom, Jones & Fischer 2001). The models in these papers indicate that the weakest core-envelope coupling that can ensure the observed near solid-body rotation in the solar interior at an age of 4.6 Gyr would produce a dispersion by a factor 2 or more in the spin rates of solar-type stars at the age of the Hyades and Coma. The observed scatter among Coma stars with mid-F to mid-G spectral types is, however, only of the order of 2 per cent. Since much of this is demonstrably caused by differential rotation, the evolutionary contribution to the scatter must be small. This argues strongly for coupling time-scales substantially shorter than the cluster age.

## 7 GYROCHRONOLOGICAL AGES OF COMA AND HYADES

The tight period–colour relation for the rotational variables found within  $12^\circ$  of the core of the Coma Berenices cluster, sharing the proper motion and lying close to the cluster main sequence, contrasts strongly with the bimodal distribution of rotation periods seen in younger clusters. The absence of a population of rapid rotators in our survey is not, however, surprising because our faint limit extends only to the boundary between K and M spectral types. In the Hyades, rapid rotation is only seen at spectral types later than our faint limit. At earlier spectral types, the period–colour relation in Coma resembles the pattern of rotation rates observed in the Hyades by Radick et al. (1987), and subsequently updated by Radick et al.

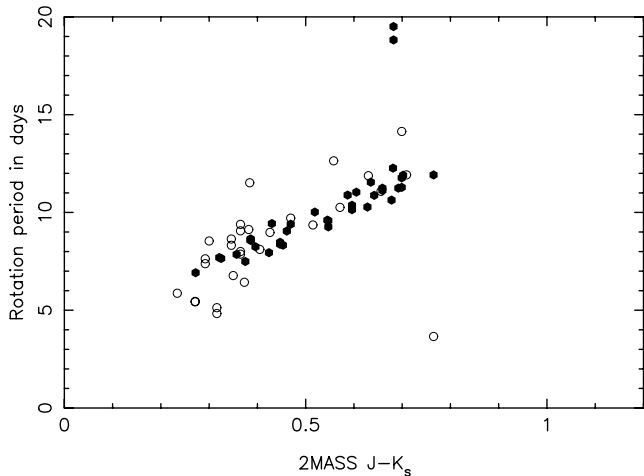


**Figure 8.** Period–colour relations for Coma Berenices (filled circles) and the Hyades (open circles). The Hyades  $J - K$  colours are taken from 2MASS, and the Hyades rotation periods from Radick et al. (1987).

(1995). In Fig. 8, we show the period–colour relations for both clusters, using 2MASS  $J - K$  colours for the Hyades stars. All but five of the Radick et al. stars were included in the *Hipparcos* survey of the Hyades by Perryman et al. (1998), and were identified as cluster members from their parallaxes, proper motions and radial velocities.

The relative rotational ages of the two clusters can be inferred from their respective period–colour relations using gyrochronology, assuming a simple rotational spin-down model. We follow a methodology similar to that of Barnes (2007), assuming the rotation period of a given star to be a separable function of age and colour. We divide the periods of stars in both clusters by the periods derived from their  $J - K$  colours at the age of Coma using equation (8). Assuming that rotation period increases as the inverse square root of age, the age of an individual star relative to the fiducial rotational age  $t_{\text{Coma}}$  of the Coma population is given by

$$t = t_{\text{Coma}} \left[ \frac{P}{9.71 + 10.68(J - K - 0.528)} \right]^2. \quad (10)$$

The relative gyrochronological ages of individual stars in the Hyades and Coma are shown as a function of  $J - K$  in Fig. 9. The sample means for the relative ages of the Coma and Hyades stars are  $1.002 \pm 0.015$  and  $1.058 \pm 0.065$ , respectively. These values exclude the lone Hyades rapid rotator with  $J - K = 0.77$ , and the anomalous slow rotator discussed above at  $J - K = 0.682$ . The difference between the gyrochronological ages of the two clusters is not statistically significant, owing to the high rms scatter in the relative age determinations for the Hyades stars. The distribution of ages for individual Coma stars is much tighter, showing an rms scatter of only 0.090 in relative age. If we adopt 625 Myr as the age of the Hyades cluster (Perryman et al. 1998), the relative gyrochronological age of Coma is found to be  $590.7 \pm 40.9$  Myr. The uncertainty is dominated by the scatter of the Hyades measurements, as seen from the cumulative distributions in Fig. 10. The mean gyrochronological age of the Coma sample is thus  $34 \pm 41$  Myr younger than that of the Hyades sample. This is in reasonable agreement with the recent comparative study of the isochrone ages of these clusters by King & Schuler (2005), who found Coma to be up to 100 Myr younger than the Hyades. Adopting  $t_{\text{Coma}} = 591$  Myr as the age of Coma, we derive the period–age–colour relation,

$$P = [9.71 + 10.68(J - K - 0.528)] \sqrt{t/591} \text{ Myr}. \quad (11)$$

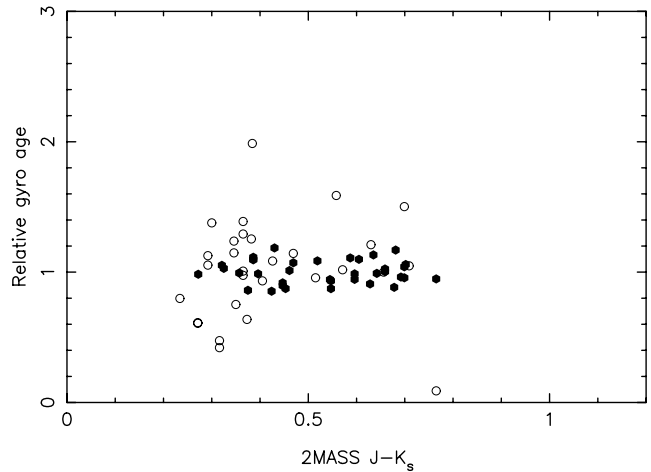


**Figure 9.** Gyrochronological ages for individual light curves of stars in Coma Berenices (filled circles) and the Hyades (open circles), derived from equation (10).

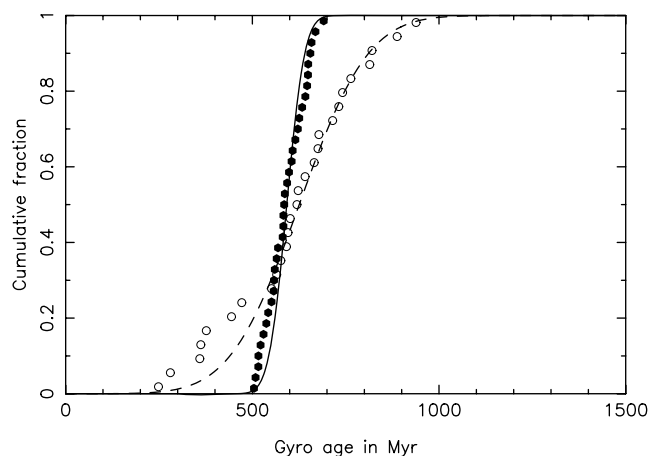


**Figure 10.** Cumulative distributions of gyrochronological ages for individual light curves of stars in Coma Berenices (filled circles) and the Hyades (open circles), derived from equation (10). The mean age of the Coma Berenices stars is 591 Myr; that of the Hyades is 625 Myr.

Equation (11) yields a predicted sidereal solar photometric modulation period of 21.8 days for an assumed  $(J - K)_{\odot} = 0.354$  (Ramírez & Meléndez 2005) and a solar age  $t_{\odot} = 4.56$  Gyr. This is shorter than the observed 26.1-day sidereal period of sunspots in the mid-latitude active belt (Donahue, Saar & Baliunas 1996). Conversely, the Sun’s 26.1-day period yields an age of 6.5 Gyr using equation (10) with  $t_{\text{Coma}} = 591$  Myr. While an idealized braking law of this kind is convenient, it is unlikely to be appropriate for real stars whose moments of inertia evolve throughout their main-sequence lifetimes. A convenient first-order correction may be a simple adjustment to the index  $b$  of the braking power law  $P \propto t^b$ , as Barnes (2007) has proposed.

The major obstacle to fine-tuning the braking power-law index is the lack of old stars with reliably determined ages and spin periods. A very few stars have already had their spin periods determined from the rotational modulation of their chromospheric Ca II H and K emission, and their ages determined from their solar-like  $p$ -mode oscillation patterns, namely  $\alpha$  Cen A and B and 70 Oph A. Barnes (2007) found  $\alpha$  Cen A and B to have comparable gyrochronological

**Table 4.**  $J - K$  colours and spin periods for the Sun and old main-sequence stars with measured rotation periods and asteroseismological age determinations.

Star	$J - K$	Period (days)	Gyro Age ( $b = 0.5$ )	Gyro Age ( $b = 0.56$ )	Seismo Age (Gyr)
Sun	0.354	$26.1 \pm 2.0$	$6.5 \pm 1.0$	$5.0 \pm 0.7$	4.57
$\alpha$ Cen A	0.35	$28.0 \pm 3.0$	$7.6 \pm 1.7$	$5.8 \pm 1.1$	$6.5 \pm 0.3$
$\alpha$ Cen B	0.49	$36.9 \pm 1.8$	$9.3 \pm 0.9$	$6.9 \pm 0.6$	$6.5 \pm 0.3$
70 Oph A	0.55	$19.9 \pm 0.5$	$2.4 \pm 0.1$	$2.0 \pm 0.1$	$6.2 \pm 1.0$
70 Oph A	0.55	$39.8 \pm 1.0$	$9.5 \pm 0.5$	$7.0 \pm 0.3$	$6.2 \pm 1.0$

*Note.* The  $J - K$  colours were determined using the effective temperatures and interpolating formulae of Ramírez & Meléndez (2005). The rotation periods are from Donahue et al. (1996) for the Sun, Barnes (2007) for  $\alpha$  Cen and from Stimets & Giles (1980) and Noyes et al. (1984) for 70 Oph A. The last row is based on the supposition that the true period of 70 Oph A is twice the measured period. The asteroseismological ages for  $\alpha$  Cen and 70 Oph A are from Eggenberger et al. (2004, 2008). The gyro ages are estimated for two different values of the magnetic braking power-law index  $b$ .

ages, from their respective spin periods of 28.0 and 36.9 days; Eggenberger et al. (2004) derived an asteroseismological age of  $6.5 \pm 0.3$  Gyr for the  $\alpha$  Cen system. The spin period of 70 Oph A was found by Stimets & Giles (1980) to be 20.1 days and by Noyes et al. (1984) to be 19.7 days from the same set of Mt Wilson Ca II H and K modulation data. Eggenberger et al. (2008) determine an asteroseismological age of  $6.2 \pm 1.0$  Gyr for 70 Oph A.

In Table 4, we show that the rotational ages of these stars are best reconciled with the asteroseismological ages by adjusting the braking power-law index from  $b = 0.5$  to 0.56. While neither value of the index  $b$  gives an age for 70 Oph A that agrees with the asteroseismological age of 6.2 Gyr at a spin period of 20 days, we note that Ca II H and K light curves can also exhibit double-peaked modulation in some seasons. It is possible that the true spin period of 70 Oph A is close to 40 days; future analyses of rotational splitting in the low-order  $p$ -modes of 70 Oph A would provide a valuable independent check on this star's rotation rate. If the longer period is correct, the asteroseismological and gyro ages can be reconciled using the same  $b = 0.56$  that fits the Sun and both components of  $\alpha$  Cen. The best-fitting period-colour-age relation is then

$$t = 591 \left[ \frac{P}{9.30 + 10.39(J - K - 0.504)} \right]^{1/0.56} \text{ Myr.} \quad (12)$$

A departure of the braking power-law index from the  $b = 0.5$  of the Skumanich relation also seems to be needed in the comparison between K dwarfs in M35 and the Hyades (Meibom et al. 2009). Hartman et al. (2009) also find that they cannot fit M37, Hyades and the Sun simultaneously with a braking law that yields an asymptotic  $t^{-1/2}$  age dependence for the stellar spin rate. Barnes (2007) and Mamajek & Hillenbrand (2008) find similar departures from the Skumanich relation in their gyrochronological age calibrations for cluster and field stars. For the purposes of the present investigation, however, the ages of the Hyades and Coma are in any case so similar that such small changes in the braking index will have little effect on the ratio of the two clusters' ages.

## 8 CONCLUSIONS

We have shown that inverse variance-weighted sine-fitting searches yield reliable period determinations from SuperWASP data in stars as faint as  $K_s = 10$ , with amplitudes of rotational variability as

low as 0.003 mag and periods of the order of 10 days recovered reliably with generalized Lomb–Scargle FAPs less than 0.01. This has enabled us to carry out the first comprehensive study of rotation among the F, G and K dwarfs in the Coma Berenices open cluster. We find a narrow, nearly linear relation between rotation period and colour from mid-F to late-K spectral types.

The scatter of the individual stellar rotation rates about the mean period-colour relation is surprisingly small, as has previously been noted by Radick et al. (1987) from their study of the Hyades, by Hartman et al. (2009) and Messina et al. (2008) from their more recent studies of M37 and by Meibom et al. (2009) from their study of M35. Indeed, our period-colour relation for Coma has a markedly lower scatter about the mean relation than Radick et al. found for the Hyades. It is not clear whether the difference in scatter is intrinsic, or simply reflects the much denser sampling of the SuperWASP observations. Some of the rotation periods in the Radick et al. Hyades sample were derived from as few as 30 observations per star obtained over an interval of 5 months. The SuperWASP periods in Coma are derived from between 1000 and 3800 observations over a 4-month period in each observing season.

The rms scatter about the mean period-colour relation in Coma is less than 5 per cent. A substantial fraction of this scatter appears to be attributable to season-to-season changes in period, caused by differential rotation and secular changes in active-region latitudes. The remaining few-per cent residuals about the fitted period-colour relation are consistent with the not-quite-complete convergence in spin rates expected from rotational models at this age. We do not see the large scatter expected from models with core-envelope coupling time-scales longer than about 100 Myr. Even solid-body spin-down models leave a residual scatter in rotation rates at the age of Coma and the Hyades. This residual scatter depends somewhat on the detailed form of the braking law among the fastest rotators at early ages, but is seldom less than about 10 per cent in the models cited above.

Although the stars in these clusters have not entirely forgotten their original spin rates, the degree of convergence is good enough to yield reasonably accurate gyrochronological age estimates. The scatter in the period-colour relation propagates into the distribution of ages for individual cluster stars derived from a linear period-colour relation assuming a simple  $t^{-1/2}$  spin-down law (Skumanich 1972). The most remarkable feature of Fig. 10 is the sharpness of the age distribution inferred for Coma. The rms scatter in the gyrochronological ages for the Coma stars is only just over 9 per cent of the mean age derived for the ensemble. This high degree of internal consistency is echoed in M37, M35 and the Hyades, as other authors have noted previously.

We have used  $J - K$  as the colour index of choice for defining a period-colour-age relation based on the Coma data, partly because of the ready availability of well-determined  $JHK$  colours in the 2MASS point-source catalogue for stars in the SuperWASP magnitude range and partly because  $J - K$  is less subject to reddening and metallicity effects than the more widely used  $B - V$  (Houlihan, Bell & Sweigart 2000). Differences in metallicity from cluster to cluster may affect the  $B - V$  colour at a given mass, and the period to which stars of a given mass converge at a given age. We raise the latter possibility because the angular momentum loss rate in a thermally driven wind depends on the wind temperature as well as the total open magnetic flux threading the wind (Mestel & Spruit 1987; Collier Cameron & Li 1994). A dependence of wind temperature on metallicity would lead to systematic differences in the asymptotic rotation rate for stars of a given mass and age in clusters with different abundances.

Despite these caveats, the relative ages derived here for Coma and the Hyades are in close agreement with the difference in their isochrone ages, even though, according to Cayrel de Strobel et al. (1997), the metallicity of Coma is subsolar by about 0.05 dex, while the Hyades is overabundant by about +0.15 dex. Our results thus support the contention of Barnes (2007) that a properly-calibrated stellar rotational clock can provide a viable means of age determination in F, G and K stars that rotate more slowly than their counterparts of the same colour in the Hyades, Coma Berenices and M37 clusters.

Some fine-tuning will still be needed to obtain gyrochronological ages of the best possible precision for main-sequence F, G and K stars. We contend that asteroseismology offers a promising way forward, providing precise measurements of both stellar ages and spin periods in mature main-sequence stars. Although such analysis is exacting and only feasible for very bright stars, it will provide valuable gyrochronological calibration standards at later ages. Gyrochronological ages can then be determined for much larger numbers of fainter stars, in a manner analogous to the cosmological distance ladder.

## ACKNOWLEDGMENTS

The WASP Consortium consists of representatives from the Universities of Keele, Leicester, The Open University, Queens University Belfast and St Andrews, along with the Isaac Newton Group (La Palma) and the Instituto de Astrofísica de Canarias (Tenerife). The SuperWASP and WASP-S Cameras were constructed and operated with funds made available from Consortium Universities and PPARC/STFC. This publication makes use of data products from the 2MASS, which is a joint project of the University of Massachusetts and the Infrared Processing and Analysis Center/California Institute of Technology, funded by the National Aeronautics and Space Administration and the National Science Foundation. This research has made use of the VizieR catalogue access tool, CDS, Strasbourg, France. We also thank the anonymous referee for insightful comments that led to substantial improvements in our methodology.

## REFERENCES

Allain S., 1998, *A&A*, 333, 629  
 Argue A. N., Kenworthy C. M., 1969, *MNRAS*, 146, 479  
 Artiukhina N. M., 1955, *Pub. Sternberg State Astron. Inst., TrSht*, 26, 3 (in Russian)  
 Baraffe I., Chabrier G., Allard F., Hauschildt P. H., 1998, *A&A*, 337, 403  
 Barnes S. A., 2007, *ApJ*, 669, 1167  
 Barnes J. R., Cameron A. C., Donati J.-F., James D. J., Marsden S. C., Petit P., 2005, *MNRAS*, 357, L1  
 Blackwell D. E., Lynas-Gray A. E., 1994, *A&A*, 282, 899  
 Carpenter J. M., 2001, *AJ*, 121, 2851  
 Casewell S. L., Jameson R. F., Dobbie P. D., 2006, *MNRAS*, 365, 447  
 Cayrel de Strobel G., Soubiran C., Friel E. D., Ralite N., Francois P., 1997, *A&AS*, 124, 299  
 Collier Cameron A., 2007, *AN*, 328, 1030

Collier Cameron A., Li J., 1994, *MNRAS*, 269, 1099  
 Collier Cameron A., Campbell C. G., Quaintrell H., 1995, *A&A*, 298, 133  
 Collier Cameron A. et al., 2006, *MNRAS*, 373, 799  
 Cumming A., 2004, *MNRAS*, 354, 1165  
 Cumming A., Marcy G. W., Butler R. P., 1999, *ApJ*, 526, 890  
 Donahue R. A., Saar S. H., Baliunas S. L., 1996, *ApJ*, 466, 384  
 Eggenberger P., Charbonnel C., Talon S., Meynet G., Maeder A., Carrier F., Bourban G., 2004, *A&A*, 417, 235  
 Eggenberger P., Miglio A., Carrier F., Fernandes J., Santos N. C., 2008, *A&A*, 482, 631  
 Girard T. M., Grundy W. M., Lopez C. E., van Altena W. F., 1989, *AJ*, 98, 227  
 Hartman J. D. et al., 2009, *ApJ*, 691, 342  
 Houdashelt M. L., Bell R. A., Sweigart A. V., 2000, *AJ*, 119, 1448  
 Irwin J., Aigrain S., Hodgkin S., Irwin M., Bouvier J., Clarke C., Hebb L., Moraux E., 2006, *MNRAS*, 370, 954  
 Keppens R., MacGregor K. B., Charbonneau P., 1995, *A&A*, 294, 469  
 King J. R., Schuler S. C., 2005, *PASP*, 117, 911  
 Krishnamurthi A., Pinsonneault M. H., Barnes S., Sofia S., 1997, *ApJ*, 480, 303  
 Li J., Collier Cameron A., 1993, *MNRAS*, 261, 766  
 Mamajek E. E., Hillenbrand L. A., 2008, *ApJ*, 687, 1264  
 Marilli E., Catalano S., Frasca A., 1997, *MmSAI*, 68, 895  
 Meibom S., Mathieu R. D., Stassun K. G., 2009, *ApJ*, 695, 679  
 Messina S., Distefano E., Parihar P., Kang Y. B., Kim S.-L., Rey S.-C., Lee C.-U., 2008, *A&A*, 483, 253  
 Mestel L., Spruit H. C., 1987, *MNRAS*, 226, 57  
 Monet D. G. et al., 2003, *AJ*, 125, 984  
 Nicolet B., 1981, *A&A*, 104, 185  
 Noyes R. W., Hartmann L. W., Baliunas S. L., Duncan D. K., Vaughan A. H., 1984, *ApJ*, 279, 763  
 Odenkirchen M., Soubiran C., Colin J., 1998, *New Astron.*, 3, 583  
 Perryman M. A. C. et al., 1997, *A&A*, 323, L49  
 Perryman M. A. C. et al., 1998, *A&A*, 331, 81  
 Pollacco D. L. et al., 2006, *PASP*, 118, 1407  
 Radick R. R., Thompson D. T., Lockwood G. W., Duncan D. K., Baggett W. E., 1987, *ApJ*, 321, 459  
 Radick R. R., Skiff B. A., Lockwood G. W., 1990, *ApJ*, 353, 524  
 Radick R. R., Lockwood G. W., Skiff B. A., Thompson D. T., 1995, *ApJ*, 452, 332  
 Ramírez I., Meléndez J., 2005, *ApJ*, 626, 465  
 Reiners A., 2006, *A&A*, 446, 267  
 Scholz A., Eislöffel J., 2007, *MNRAS*, 381, 1638  
 Skumanich A., 1972, *ApJ*, 171, 565  
 Stauffer J. R., Hartmann L. W., 1987, *ApJ*, 318, 337  
 Soderblom D. R., Jones B. F., Fischer D., 2001, *ApJ*, 563, 334  
 Stimets R. W., Giles R. H., 1980, *ApJ*, 242, L37  
 Tamuz O., Mazeh T., Zucker S., 2005, *MNRAS*, 356, 1466  
 Trumpler R. J., 1938, *Lick Obs. Bull.*, 18, 167  
 Urban S. E., Corbin T. E., Wycoff G. L., 1998, *AJ*, 115, 2161  
 van Leeuwen F., 1999, *A&A*, 341, L71  
 Wolff S. C., Strom S. E., Hillenbrand L. A., 2004, *ApJ*, 601, 979  
 Zacharias N., Monet D. G., Levine S. E., Urban S. E., Gaume R., Wycoff G. L., 2005, *VizieR On-line Data Catalog*, 1297, 0  
 Zechmeister M., Kürster M., 2009, *A&A*, 496, 577

This paper has been typeset from a  $\text{\TeX}/\text{\LaTeX}$  file prepared by the author.